

Development of COVID-19 Booster Vaccine Policy by Microsimulation and Q-learning¹

Guoxuan Ma, M.S., Department of Biostatistics, University of Michigan, Ann Arbor, United States

Lili Zhao², Ph.D., Feinberg School of Medicine, Northwestern University, Chicago, United States

Jian Kang³, Ph.D., Department of Biostatistics, University of Michigan, Ann Arbor, United States

Keywords: Vaccine Policy, Public Health, Q-learning, Recurrent Neural Network, Vaccine booster

¹This manuscript is under review of the *Journal of American Statistical Association*

²Corresponding author. Postal address: 1400, 680 North Lake Shore, Chicago, IL 60611-4407, United States. Email: zhaolili@northwestern.edu. Phone number: (+1) 734-353-1652

³Corresponding author. Postal address: 1415 Washington Heights, Ann Arbor, MI 48109-2029, United States. Email: jiankang@umich.edu. Phone number: (+1) 734-763-1607

Abstract

Objectives: To develop a novel framework for effective and interpretable booster vaccination policymaking without real-world interaction, addressing both ethical and exploration challenges in public health vaccine policymaking.

Materials and Methods: We propose a framework combining online tabular Q-learning with an RNN-based environment that interacts with the Q-learning agent. With electronic health record data from Michigan Medicine, we train a Recurrent Neural Network (RNN) to capture the complex temporal association between infection status and patients' characteristics and enable the simulation of individual trajectories. Then, we perform online tabular Q-learning, where the Q-function is modeled as a table, for vaccine policy learning based on the RNN microsimulator to avoid the need of actual executing the decision on whether to receive the vaccination.

Results: The RNN-based environment simulator can simulate data with very similar marginal and conditional infection rates with those in the real data. The proposed Q-learning-based policy outperformed current observed vaccination strategies when applied to COVID-19 booster policies. The resulting policy table is interpretable and effectively balances the trade-offs between infection risks and vaccine side effects, leading to improved outcomes compared to existing practices.

Discussion and Conclusion: The combination of Q-learning and microsimulation provides a powerful framework for vaccine policy development, avoiding the ethical and practical challenges of real-world RL exploration. The framework offers a path toward more effective and data-driven vaccination strategies.

1 Introduction

The COVID-19 pandemic underscored the critical importance of rapid and effective vaccination strategies to control the spread of the virus and minimize the burden on healthcare systems. However, developing optimal vaccination policies for public health is fraught with challenges. Clinical trials do not have sufficient data to evaluate vaccine policies comprehensively, as they often enroll subjects with specific characteristics that may not be representative of the general population (Jüni et al., 2001; Lander et al., 2019). As a result, the findings from these trials may not always generalize well to the broader population, potentially hindering the development of comprehensive vaccination policies. For instance, people taking immunosuppressant medications were excluded from the trials developing BNT162b2 (Pfizer-BioNTech) and mRNA-1273 (Moderna) vaccines (Polack et al., 2020; Baden et al., 2021). The lack of data in this group regarding the vaccines efficacy has prevented the development of an effective vaccine policy against COVID-19 infections for immunosuppressed patients (Risk et al., 2022). Moreover, conducting large-scale randomized trials on vaccine policy evaluation during a pandemic poses significant ethical challenges. Randomizing subjects to the group that do not receive the vaccine can place participants at increased risk of COVID-19 infection, raising ethical concerns about exposing groups of people to potential harm (Adebamowo et al., 2014; Monrad, 2020). These challenges highlight the need for alternative approaches to develop and improve vaccine policies using existing real-world data while adhering to safety and ethical standards.

Reinforcement learning (RL) offers a promising framework for developing treatment strategies for diseases and has been successfully applied in various fields in healthcare (Sutton and Barto, 2018; Yu et al., 2021), including cancer treatment (Beerenwinkel et al., 2015; Tseng et al., 2017), glucose regulation (Yasini et al., 2009; Sun et al., 2018), HIV treatment (Yu et al., 2019),

and mental diseases intervention (Laber et al., 2014), but it has not been widely adopted in public health (Weltz et al., 2022). In an RL setup, an agent selects actions based on its current state, receiving feedback (rewards) and the new state from the environment. The objective is for the agent to learn an optimal policy, which is a mapping from states to actions, that maximizes the cumulative reward over time. RL is particularly suited for systems with inherent delays, where decisions are made sequentially without immediate feedback and are evaluated based on long-term outcomes. This makes RL a compelling approach for developing effective policies in public health, including policymaking in vaccination, where the health outcomes are often evaluated based on a prolonged period with delayed feedback (Yu et al., 2021).

However, RL agents do not receive explicit instructions on which actions to take; instead, they learn the best actions through trial and error (in the online setting) or learn from the existing data (in the offline setting). While the online trial-and-error process encourages agents to explore new policies that are potentially effective, applying this approach directly in real-world scenarios can raise ethical concerns (Levine et al., 2020). Early in the training process, the trial-and-error learning mechanism often lead to suboptimal or even harmful decisions, potentially causing harm to subjects before corrective feedback is obtained. While this may be less problematic in applying RL in Dynamic Treatment Regimes (DTR) (Liu et al., 2017; Zhang, 2020; Guo et al., 2022), where treatment decisions are usually made under experts' supervision to ensure the decisions are clinically relevant and safe, it becomes more critical in scenarios of learning vaccine policy during a global pandemic like COVID-19, where it is impossible to provide individualized supervision for the whole population. In such cases, incorrect vaccination timing or administration could lead to severe infections or serious adverse effects. This problem in online training can be resolved by an offline approach, where actions are learned based on observed data. However, the offline approach may struggle with exploring new policies that could lead to potential improvements and cannot effectively learn from the observed offline

data (Levine et al., 2020). Moreover, it faces the same ethical concerns when evaluating the learned policy in real world with the absence of proper supervisions. Therefore, there is a need to develop an online RL framework based on existing data without direct interactions with the real world.

Q-learning is a Reinforcement Learning algorithm that helps agents learn how to make decisions by evaluating the potential value of different actions in various states (Watkins and Dayan, 1992). It maintains a Q-function of the state-action pairs, which represents the expected future reward of taking a particular action in a given state. To determine the best action for a given state, the agent examines the Q-values associated with all possible actions and selects the one with the highest value. The Q-value for each state-action pair is initially designed to be stored explicitly in a table, as seen in tabular Q-learning (Watkins and Dayan, 1992). Later, deep neural networks (DNN) are often used to model the Q-function for its flexibility and ability to accommodate continuous state and action spaces (Mnih et al., 2015; Liu et al., 2017; Raghu et al., 2017; Yu et al., 2021). While deep Q-learning is useful in precision medicine or individualized treatment where state and action spaces are often large or continuous (Liu et al., 2017; Zhang, 2020; Guo et al., 2022; Wu et al., 2023), public health problems can be effectively represented with a finite and discrete set of states and actions, policies are often applied to groups of people rather than being tailored to individual subjects. Moreover, unlike tabular Q-learning, deep Q-learning lacks theoretical convergence guarantees to the global optimum due to the complexities of neural networks and function approximation and often suffers from convergence difficulties (Watkins and Dayan, 1992; Van Hasselt et al., 2016; Fan et al., 2020).

To address these challenges, we propose a framework combining online tabular Q-learning with an RNN-based environment that interacts with the Q-learning agent. We refer to this RNN-based environment as a microsimulation model (Rutter et al., 2011; Julien et al., 2022), as it effectively simulates individual trajectories and creates a virtual environment that mirrors

real-world dynamics. Figure 1 provides an illustration. While our framework is useful in general public health policymaking, we focus on COVID-19 vaccine policy in this paper. We train an Recurrent Neural Network (RNN) with the Long-Short Term Memory (LSTM) architecture, which has been widely used to model sequential data and has successful applications on modeling the relationship between COVID-19 infections and vaccinations (Sherstinsky, 2020; Shen et al., 2024), to capture the complex temporal association between infection status and patients’ characteristics. Then, we perform online tabular Q-learning, where the Q-function is modeled as a table, for vaccine policy learning based on the RNN microsimulator to avoid the need of actual executing the decision on whether to receive the vaccination.

Our approach has two key contributions. First, by employing an RNN with the LSTM architecture, we create a microsimulation model as the virtual environment used in RL that can generate data for individuals that closely resembles real-world data, while accounting for the inherent uncertainty. The RNN-based microsimulator not only avoids ethical concerns but also provides an unlimited amount of data for training, which facilitates the creation of “what if” scenarios, allowing us to evaluate different policies on simulated individuals with the same characteristics during the same period of time. Second, by using the tabular Q-learning, our approach produces a clear and interpretable policy table where Q-values for different actions and various groups of people can be easily read. We define the reward function by balancing the risk of severe infections and the potential side effects of the vaccination. In this paper, we focus on the vaccination policy for the COVID-19 booster dose, i.e., whether and when different groups of people should receive the booster after the second COVID-19 vaccination. The policy derived from our Q-table demonstrates superior performance compared to the current observed policy, indicating significant potential for improvement if the learned policy is adopted.

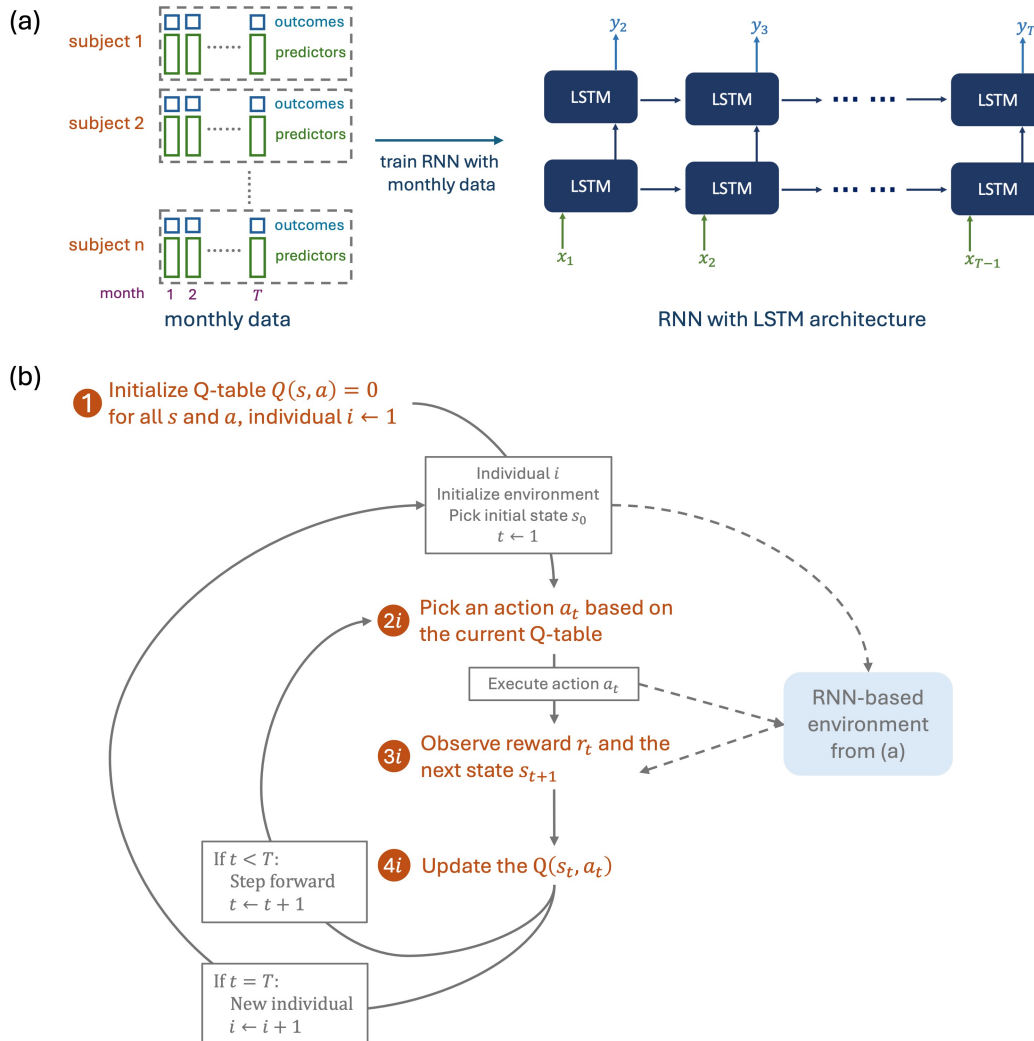


Figure 1: The Q-learning framework with an RNN environment simulator. (a) Creating environment simulator for individual trajectory. We train an RNN with 2-stacked LSTM layers using monthly EHR data. For one subject, x_t represents predictors in month t for $t = 1, \dots, T - 1$, and y_t presents the outcomes, i.e., the severe infection and general infection status, in month t for $t = 2, \dots, T$. (b) Steps of online tabular Q-learning. The RNN-based environment is based on the fully-trained RNN with LSTM architecture in (a).

2 Materials and Methods

2.1 Data overview

We use electronic health record (EHR) from Michigan Medicine (study ID: HUM00164771). The data includes health records of patients, including demographics, COVID-19 vaccination dates, COVID-19 infection dates and other baseline information, for 122,4147 patients. We

include patients with a primary care physician and received at least one COVID-19 test at the University of Michigan Hospital. We exclude patients with race and gender missing. A total of 81,000 patients are included in this study. The primary outcome we consider is whether the patient has severe COVID-19 infection (requiring hospitalization), and the secondary outcome is whether the patient has general COVID-19 infection. In this study, we summarize monthly data from the original EHR data starting from March 2020, and a patient’s record terminates either at June 2022, the month of severe infection or decease, whichever comes first. The maximum span of data sequence for a patient is $T = 27$ months, from March 2020 to June 2022.

2.2 Methods

Let $\{s_t\}_{t \geq 0}$ be a Markov process with state space \mathcal{S} representing an individual’s baseline characteristics, vaccination history and severe infection status at each month. Let a_t represent the choice to receive a booster or not in month t with action space $\mathcal{A} = \{0, 1\}$. For $s, s' \in \mathcal{S}$ and $a \in \mathcal{A}$, denote by $P(s'|s, a) = \Pr(s_{t+1} = s' \mid s_t = s, a)$ the state transition probability function, and by $r(s, a)$ the reward function that assigns a reward of taking action a in the state s . Then, we model the decision-making process of whether an individual should receive a booster at each month as a Markov Decision Process (MDP), denoted by $\mathcal{M} = \{\mathcal{S}, \mathcal{A}, P, r\}$. In this framework, the current state adequately summarizes the past, meaning future states are independent of past states given the current state and action. This assumption entails little loss of generality mathematically because almost any decision process can be reformulated as an MDP by appropriately aggregating the historical data (Sutton, 1997; Wetz et al., 2022).

In Reinforcement Learning (RL), an agent interacts with the environment to improve its decision-making ability over time. An agent is a decision-maker responsible for determine whether an individual should receive a COVID-19 booster shot. The agent selects an action

based on the current state according to a policy $\pi : \mathcal{S} \mapsto \mathcal{A}$, which maps a patient’s health status, vaccination history, and other relevant information (a state) to an action (whether to administer a booster or not). The environment, on the other hand, consists of the state transition function $P(s'|s, a)$ and the reward function $r(s, a)$. The environment interacts with the agent by providing the next state and reward after each action is taken.

We first introduce the Q-learning framework to derive an good policy for booster vaccination, assuming the environment is known. However, due to ethical concerns around allowing an agent to directly interact with real-world patients in the development of COVID-19 booster polices, we construct a microsimulation model as a virtual environment using RNN trained on existing patient data. Algorithm 1 outlines the steps of online tabular Q-learning in the RNN-based environment in our application of booster policy development.

2.2.1 Booster policy learning by tabular Q-learning

We perform online tabular Q-learning given a known environment. The objective is to find a policy π^* that maximizes the expected cumulative reward, defined by the value function,

$$V^\pi(s_0) = \mathbb{E}_{\{s_t\}_{t \geq 0}} \left[\sum_{t=0}^{\infty} \gamma^t r \{s_t, \pi(s_t)\} \right],$$

where $V^\pi(s_0)$ represents the expected cumulative reward starting from an initial state s_0 by following a policy π , and $\gamma \in (0, 1]$ is the discount factor on future reward. The expectation is taken over possible trajectories of the Markov process $\{s_t\}_{t \geq 0}$ generated by the policy π starting from the initial state s_0 . Since we operate under the MDP framework with an infinite time horizon, the value function is stationary. This means that for any state, its value remains constant over time, as the recursive nature of the decision-making process ensures that the value depends only on the current state, not on when it is encountered.

Algorithm 1 Online tabular Q-learning in RNN based environment simulator

```
1: Initialize Q-table  $q(s, a) = 0$  for all  $s$  and  $a$ 
2: Initialize  $\epsilon = 0.5$  and  $\beta = 0.001$ , fix  $\gamma = 0.99$ ,  $\lambda_\epsilon = 0.99$ ,  $\lambda_\beta = 0.998$ , and  $k_\epsilon = k_\beta = 5000$ ,
   which are commonly used values (Sutton and Barto, 2018)
3: for individual  $i$  in  $1 : n$  do
4:   Extract age, immunosuppressant usage, and the month of the second vaccination  $T_i$  for
   individual  $i$  from EHR data
5:   Set months since the last vaccine to 0 for individual  $i$ 
6:   Initialize state  $s_0$  with age, immunosuppressant usage and months since the last vaccine
   for individual  $i$ 
7:   for time  $t$  in  $T_i + 1 : T$  do
8:     if  $t - T_i \leq 4$  then
9:       Select  $a_t = 0$  by following the CDC guideline
10:    else
11:      Select random action  $a_t$  with probability  $\epsilon$ , otherwise select  $a_t = \arg \max_a q(s_t, a)$ 
12:    end if
13:    Obtain  $r_t, s_{t+1}$  and  $I_{t+1}$  from the RNN micro-simulated environment; collect transition
    $(s_t, a_t, r_t, s_{t+1})$ 
14:    Update  $q(s_t, a_t) \leftarrow q(s_t, a_t) + \beta \left( r_t + \gamma \max_a q(s_{t+1}, a) - q(s_t, a_t) \right)$ 
15:    if  $I_{t+1} = 1$  then
16:      Terminate simulation for individual  $i$ , continue to the next individual
17:    end if
18:    Decay  $\epsilon \leftarrow \lambda_\epsilon \epsilon$  every  $k_\epsilon$  steps, decay  $\beta \leftarrow \lambda_\beta \beta$  every  $b_\beta$  steps
19:  end for
20: end for
```

Under the MDP framework, the optimal policy π^* satisfies the Bellman equation,

$$V^*(s) = \max_{\pi} \mathbb{E} [r \{s, \pi(s)\} + \gamma V^*(s')],$$

where s is the current state and s' is the next state. Q-learning provides a framework for solving this Bellman equation by estimating the Q-function,

$$q(s, a) = \mathbb{E} [r(s, a) + \gamma V^*(s')],$$

where $q(s, a)$ represents the value of taking action a in state s . The optimal action at any state s can then be determined by taking $\arg \max_a q(s, a)$. Since the Q-function is initially unknown, we model it as a table, where each cell (s, a) holds the estimated value of $q(s, a)$ (Watkins and Dayan, 1992). The Q-learning algorithm takes an iterative approach to updating the Q-table:

after each interaction with the environment, we adjust $q(s, a)$ based on the observed reward r and the estimated future value by the following updating rule (Watkins and Dayan, 1992),

$$q(s, a) \leftarrow q(s, a) + \beta \left\{ r + \gamma \max_u q(s', u) - q(s, a) \right\}$$

where β is a prespecified learning rate and s' is the next state.

In this study, we aim to learn a policy on whether and when to receive a COVID-19 booster, so we only consider subjects with at least two COVID-19 vaccinations and their trajectories after their second vaccinations. At any month t , we decide the state $s_t \in \mathcal{S}$ consists of four relevant variables: age (categorical, 18-29/30-49/50-64/65+), baseline immunosuppressant usage (binary), months since the last vaccination (categorical, 0-4/5-6/7+), and the severe infection status (binary). The action $a_t \in \mathcal{A} = \{0, 1\}$ indicates whether or not a booster is received. In this study, we follow the Centers for Disease Control and Prevention (CDC) guidelines that an additional COVID-19 vaccine should be at least 4 months following the previous dose. The guideline was for adult ages 65 years and older but we generalize it to all age groups for simplicity. Following this guideline, a_t is constrained to be 0 regardless of the values in Q-table for t within 4 months of the second vaccination.

2.2.2 Creating the environment through microsimulation

The RL environment is characterized by two key components: the state transition rules and the reward function. We simulate state transitions using RNN, enabling the microsimulation of individual trajectories. The reward function is designed to balance the risk of severe infection with potential adverse effects of a COVID-19 booster.

Microsimulation of state transitions Let w_t represent a set of additional variables relevant to the individual’s profile, though of less interest to the vaccine policy decision and not included in the state variable s_t . It includes an individual’s baseline and time-varying charac-

teristics. In this study, baseline characteristics include gender (Female/Male), race (categorical, Caucasian/African American/Others), baseline number of visits to hospital (categorical, 0/5-9/10-19/20-49/50+), and baseline Charlson comorbidity (categorical, 0/1-2/3-4/5+) (Charlson et al., 1987; Gasparini, 2018). The baseline period is one year before the study period starts, i.e., from March 1, 2019 to February 29, 2020. Time-varying variables include COVID-19 variant (categorical, Alpha/Delta/Omicron) and total number of vaccinations received up to month t (integer, 0-4).

We train an RNN with LSTM units to approximate the transition dynamics between states. Conceptually, for month $t = 1, \dots, T - 1$, let $x_t = [s_t, w_t, a_t]$ denote the RNN predictors and $y_{t+1} = [s_{t+1}, w_{t+1}]$ denote the RNN outcomes. The RNN takes as input the sequence of predictors x_1, \dots, x_t and predicts the outcome y_{t+1} . The transition dynamics from $[s_t, w_t]$ to $[s_{t+1}, w_{t+1}]$ given action a_t are modeled by the fully trained RNN, from where we obtain the transition dynamics from s_t to s_{t+1} .

In this study, certain state variables, including age, baseline immunosuppressant usage and months since the last vaccination, as well as the set of additional variables w_t are deterministic given action and time. Therefore, these variables are excluded from the outcomes, as their transitions are fixed. Additionally, since severe infections are treated as a terminal event (i.e., the trajectory is terminated upon a severe infection), severe infection status is always zero in s_t for month t before termination. As the general infection is an important variable that affects the likelihood of severe infection, we include the binary general infection status besides the binary severe infection status into the outcome variable. The output layer of the RNN uses a sigmoid activation to predict the probability of infections in the next month. This allows us to sample transitions from s_t to s_{t+1} based on the underlying state transition function, and realize microsimulation of individual trajectories in alignment with the Q-learning policy. Section 3.1 shows that the state transition probabilities estimated from the microsimulated individuals

match well with those evaluated on real-data.

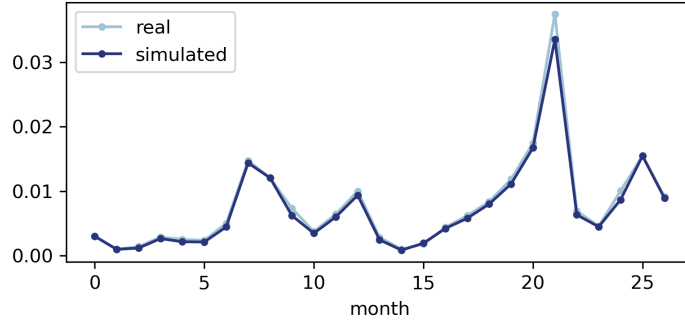
Define rewards We define the reward in month t , given state s_t and action a_t , as:

$$r_t(s_t, a_t) = -I_{t+1}(s_t, a_t) \times (1 + \alpha \times a_t), \quad (1)$$

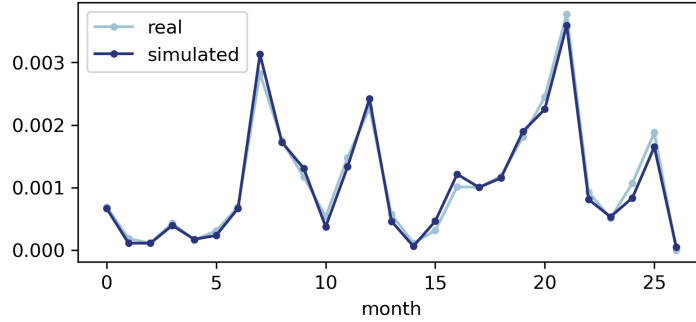
where $I_{t+1}(s_t, a_t) : \mathcal{S} \times \mathcal{A} \rightarrow \{0, 1\}$ is the severe COVID-19 infection status for the next month, and α represents the relative cost of receiving a booster. The next-month severe COVID-19 infection status $I_{t+1}(s_t, a_t)$ can be sampled using the probability generated by the fully trained RNN. The reward consists of two components: the predicted risk of severe infection in the next month and the potential side events of the booster. The parameter α quantifies the perceived harm of receiving a booster relative to the risk of a severe infection. As the Q-learning seeks a policy to maximize the expected cumulative reward, when α is small, it is likely to recommend boosters for all groups due to protective effect of vaccines against severe infections. Conversely, a large α may result in a policy that discourages booster administration, as the perceived harm outweighs the infection risk. In practice, the choice of α should reflect the relative importance placed on the risk of infection versus the harm of vaccination. We discuss our choice of α in Section 3.2.1 when presenting our results.

3 Results

In this section, we first present results of our microsimulations, showing that our RNN-based environment resembles real data well in terms of both marginal infection probabilities and conditional infection probabilities. Then, we present our Q-learning results, showing that the Q-table-based policy has an advantage over other policies in terms of rewards. We interpret the Q-table-based policy on whether and when to receive the booster on different groups of population when choosing selected vaccine costs.



(a) Marginal general infection rate by month.



(b) Marginal severe Infection rate by month.

Figure 2: Marginal general infection rate and marginal severe infection rate by month summarized from the simulated data and the real data.

3.1 Microsimulation to create environment

We train the RNN using monthly data of the 81,000 patients starting from March 2020 to June 2022. We use an RNN with 2 stacked LSTM layer for training. Each LSTM layer has 128 hidden nodes with dropout rate 0.2 (Srivastava et al., 2014). During training, we use the Adam optimizer with learning rate 10^{-4} for 2,000 epochs (Kingma and Ba, 2014). To evaluate the RNN-based environment, we simulate a data sequence starting from the predictors at March 2020 for each of the 81,000 patients by the trained RNN. We summarize the severe infection rate and the general infection rate from the simulated data and compare them with the real EHR data.

The simulated population marginal general infection rate and marginal severe infection rate over the 27 months are 7.25‰ and 1.06‰ respectively, which are close to the observed values

Table 1: Severe infection rate (%o) conditional on one variable: (a) age (b) number of previous COVID-19 vaccines (c) number of baseline hospital visits (d) comorbidity score.

(a) Age			(b) Number of vaccines		
	Simulated	Real		Simulated	Real
Age [0, 18)	0.67	0.67	numVax = 0	1.27	1.28
Age [18, 30)	0.92	1.06	numVax = 1	1.04	1.06
Age [30, 50)	1.07	1.12	numVax = 2	0.72	0.73
Age [50, 65)	1.14	1.05	numVax = 3	0.73	0.85
Age 65+	1.26	1.26	numVax = 4	0.32	1.00

(c) Number of visits			(d) Comorbidity		
	Simulated	Real		Simulated	Real
numVisits [0, 5)	0.76	0.79	Comorbidity [0, 1)	0.76	0.77
numVisits [5, 10)	0.74	0.75	Comorbidity [1, 3)	1.43	1.39
numVisits [10, 20)	1.08	1.05	Comorbidity [3, 5)	2.18	2.24
numVisits [20, 50)	1.84	1.76	Comorbidity 5+	3.02	3.15
numVisits 50+	2.84	3.28			

in real data (7.91%o and 1.06%o respectively). Figure 2 shows the marginal general infection rate and marginal severe infection rate within the population at each month for the simulated data and the real data. The RNN-based environment fits very well both the marginal general infection rate and marginal severe infection rate within the population over the 27 months. The simulated marginal infection rates is very close to the real infection rates at each month.

Table 1 shows the severe infection rate conditional on one variable and Table 2 shows the severe infection rate conditional on multiple variables. The simulated conditional severe infection rate is very close to the rates observed in real data in most cases. Rarely, the simulated conditional severe infection rate has some difference with the observed values because there are limited data points within that category.

Overall, results show that the RNN-based environment simulator is reliable for the online tabular Q-learning. The trained RNN can simulate data with very similar marginal and conditional infection rates with those in the real data. It well captures the relationship between the infection status and both the baseline and time-varying variables.

Table 2: Severe infection rate (simulated/real, %) conditional on multiple variables: (a) Baseline immunosuppressant status and gender (b) COVID variant and race.

(a) Baseline immunosuppressant status and gender.

	imm_baseline = 0	imm_baseline = 1
gender = 0	0.95 / 0.95	1.53 / 1.51
gender = 1	1.01 / 1.05	2.02 / 1.85

(b) COVID variant and race

	Variant None	Variant Delta	Variant Omicron
Race Caucasian	0.76 / 0.76	1.56 / 1.53	0.72 / 0.79
Race African American	1.71 / 1.61	4.60 / 4.57	1.30 / 1.55
Race Others	0.75 / 0.80	1.60 / 1.69	0.71 / 0.76

3.2 Booster policy learning

We include three variables in state \mathcal{S} in the online tabular Q-learning: age, baseline immunosuppressant status, and number of months to the second COVID-19 vaccination. Since we aim to learn a policy on whether to receive a COVID-19 booster at a specific month, we only consider subjects with at least two COVID-19 vaccinations. In this study, we focus on the policy of the first booster.

3.2.1 Reward evaluation

We compare the population average rewards over months of the Q-table-based policy and three other policies – policy from data, receiving a booster, and never receiving a booster. For the policy from data, we extract whether and when each subject received the first booster from the real data. For the policy of receiving a booster, we randomly pick a month between the 5th from the second vaccination and the last month of the study for each subject to receive a booster. For the policy of never receiving a booster, no one receives any booster at any month. We train the Q-table for 30 epochs and repeat the training 20 times with different random seeds. Supplementary Materials S1 shows that the tabular Q-learning algorithm converges before 30

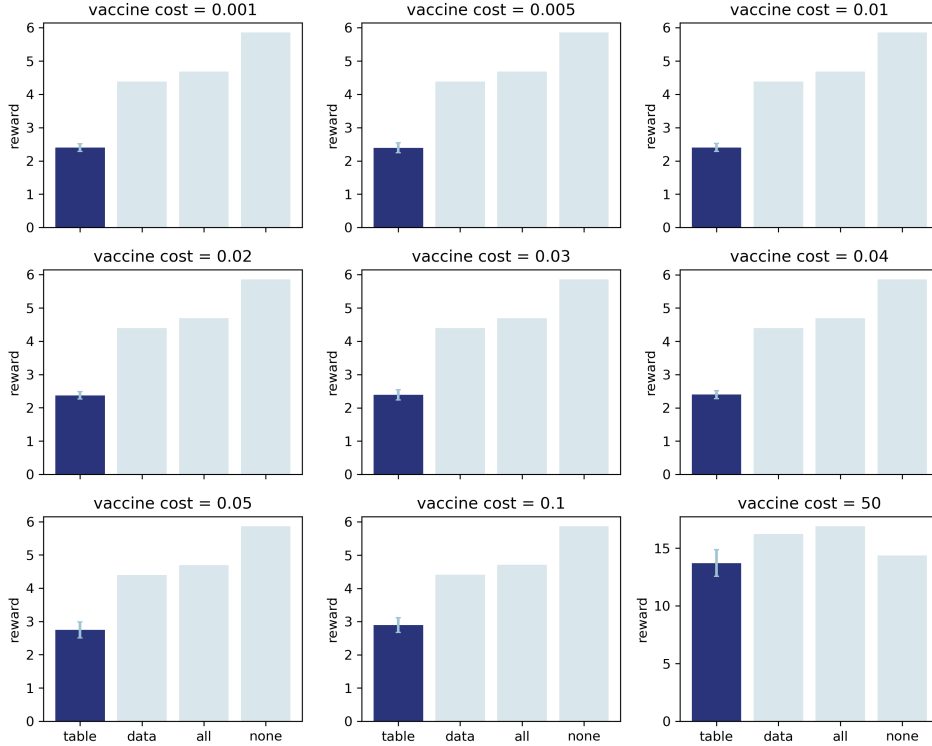


Figure 3: Negative rewards ($\times 10^{-4}$) for the Q-table-based policy (table), the policy from data (data), the policy of always receiving a booster (all), the policy of never receiving a booster (none). The error bar represents mean \pm s.d. of the population average negative rewards over the 20 replicates for the Q-table-based policy.

epochs in our study. The discount factor γ in the tabular Q-learning is fixed at 0.99.

The vaccine cost α is an important hyperparameter that controls the belief of the relative harmness of a severe infection and the booster. One of the choice is to determine a reasonable range of vaccine cost based on mortality rates after a severe infection and the booster. We compute the mortality rate after 30 days among people who received the booster (0.04%) and the mortality rate after 30 days among people who had a severe infection (1.05%) from the real data. We use the ratio (0.04) of the two mortality rates for a proxy of the relative risk of a booster to a severe infection, so we primarily focus on the vaccine cost α around 0.04.

Figure 3 shows the negative rewards (the lower the better) for the four policies and selected vaccine costs around 0.04. For all the vaccine costs, the Q-table-based policy consistently has the highest reward. The Q-table-based policy has a stable reward over the 20 replicates. When

the vaccine cost increases (vaccine cost = 50), the Q-table-based policy gets close to the policy of never receiving a booster, as the large vaccine cost discourages it to receive a booster at any time point. It is worth-noting that the Q-table-based policy has a higher reward than the policy from the real data in all cases. This indicates the policy that was followed by the general population is sub-optimal and could have been improved by our Q-table-based policy.

In Supplementary Materials S2, we provide the comparison between tabular Q-learning and deep Q-learning under different vaccine costs. Results show that deep Q-learning with various combinations of architectures and learning rates suffers from convergence difficulties and stability issues. This highlights the practical advantage of tabular Q-learning over deep Q-learning in this application.

3.2.2 Policy interpretation

In Section 3.2.1, we determine 0.04 as a reasonable vaccine cost based on the mortality rates ratio after 30 days of a booster and a severe infection. Based on the 20 replicates, we obtain a confidence measure for receiving booster of the Q-table-based policy. We determine a group of people need to receive the booster if more than 10 replicates out of the 20 suggest so (i.e., confidence measure for receiving booster is bigger than $10/20 = 0.5$).

When vaccine cost is 0.04, adults of all age groups, regardless of the baseline immunosuppressant status are suggested to receive the COVID-19 booster after 5-6 months of the second vaccination. When vaccine cost decreases to 0.03, the policy remains the same but the confidence measure for most groups of people increases to at least 0.9. However, if the vaccine cost increase to 0.05, the Q-table-based policy suggests people of age 50-65 without the baseline usage of immunosuppressant not receiving the booster until the 7th month after the second vaccination, while people within the same age group but have used immunosuppressant should receive the booster after 5-6 months of the second vaccination. People of age 30-50 without

baseline immunosuppressant usage are suggested to receive the booster 5-6 month after the second vaccination, while people within the same age group who have used immunosuppressant during baseline period are not suggested to receive the vaccine until the 7th month after the second vaccination. Adults of all other age groups are suggested to take the booster after 5-6 months after the second vaccination. The policy does not change but the confidence measure for receiving booster are generally lower if vaccine cost rises to 0.1.

4 Discussion and Conclusion

In this paper, we propose a novel framework combining tabular Q-learning with an RNN-based environment simulator to optimize COVID-19 booster vaccination policies. The proposed approach addresses key challenges in vaccine policy development, including the limitations of clinical trials and ethical concerns on need of direct interactions of the Reinforcement Learning (RL) algorithms with the real world. By utilizing an RNN with LSTM architecture, we successfully model the temporal relationships of COVID-19 infections and vaccination status, generating simulated data that reflects real-world dynamics. The policy learned through our method outperforms the currently observed practices of COVID-19 booster vaccination, indicating its potential to enhance vaccine deployment and reduce infection rates.

Our framework offers several advantages. First, the RNN-generated simulated data enables continuous exploration of potential policies without ethical concerns. This allows us to conduct extensive policy evaluations without requiring real-world interventions, avoiding the risks of harmful or suboptimal decisions. Second, by employing tabular Q-learning, we provide an interpretable and clear policy table, allowing policymakers to easily understand and implement optimal vaccination strategies. While Deep Q-learning has been widely applied in healthcare for its flexibility in large state spaces, it suffers from convergence difficulties and stability issues

in our applications (see Supplementary Materials S2). This instability highlights the value of tabular Q-learning, which, while simpler, offers more reliable and interpretable outcomes for public health problems where states and actions are discrete.

This research demonstrates the effectiveness of RL in public health policy development and presents a scalable solution for future pandemics or vaccine rollouts. While our application focused on COVID-19 booster policies, the framework can be generalized to the development and improvement of other public health decisions.

Acknowledgement

This study was partly funded by the National Institute of Allergy and Infectious Diseases of the National Institutes of Health under Award Number R01AI158543. The funder played no role in study design, data collection, analysis and interpretation of data, or the writing of this manuscript.

Contribution Statement

All authors conceptualize the project and develop the methodologies. Guoxuan Ma is responsible for data curation, analysis, coding, investigation, validation, visualization and write the original draft. Both Lili Zhao and Jian Kang are responsible for computing resources, supervision, reviewing and editing the manuscript.

References

- Adebamowo, C., Bah-Sow, O., Binka, F., Bruzzone, R., Caplan, A., Delfraissy, J.-F., Heymann, D., Horby, P., Kaleebu, P., Tamfum, J.-J. M., et al. (2014). Randomised controlled trials for ebola: practical and ethical issues. *The Lancet* **384**, 1423–1424.
- Baden, L. R., El Sahly, H. M., Essink, B., Kotloff, K., Frey, S., Novak, R., Diemert, D., Spector, S. A., Roupheal, N., Creech, C. B., et al. (2021). Efficacy and safety of the mrna-1273 sars-cov-2 vaccine. *New England Journal of Medicine* **384**, 403–416.
- Beerenwinkel, N., Schwarz, R. F., Gerstung, M., and Markowetz, F. (2015). Cancer evolution: mathematical models and computational inference. *Systematic Biology* **64**, e1–e25.
- Charlson, M. E., Pompei, P., Ales, K. L., and MacKenzie, C. R. (1987). A new method of classifying prognostic comorbidity in longitudinal studies: development and validation. *Journal of Chronic Diseases* **40**, 373–383.
- Fan, J., Wang, Z., Xie, Y., and Yang, Z. (2020). A theoretical analysis of deep q-learning. In *Learning for Dynamics and Control*, pages 486–489. PMLR.
- Gasparini, A. (2018). comorbidity: An r package for computing comorbidity scores. *Journal of Open Source Software* **3**, 648.
- Guo, H., Li, J., Liu, H., and He, J. (2022). Learning dynamic treatment strategies for coronary heart diseases by artificial intelligence: real-world data-driven study. *BMC Medical Informatics and Decision Making* **22**, 39.
- Julien, J., Ayer, T., Tapper, E. B., Barbosa, C., Dowd, W. N., and Chhatwal, J. (2022). Effect of increased alcohol consumption during covid-19 pandemic on alcohol-associated liver disease: a modeling study. *Hepatology* **75**, 1480–1490.

- Jüni, P., Altman, D. G., and Egger, M. (2001). Assessing the quality of controlled clinical trials. *BMJ* **323**, 42–46.
- Kingma, D. P. and Ba, J. (2014). Adam: A method for stochastic optimization. *arXiv preprint arXiv:1412.6980* .
- Laber, E. B., Linn, K. A., and Stefanski, L. A. (2014). Interactive model building for q-learning. *Biometrika* **101**, 831–847.
- Lander, J., Langhof, H., and Dierks, M.-L. (2019). Involving patients and the public in medical and health care research studies: An exploratory survey on participant recruiting and representativeness from the perspective of study authors. *PloS One* **14**, e0204187.
- Levine, S., Kumar, A., Tucker, G., and Fu, J. (2020). Offline reinforcement learning: Tutorial, review, and perspectives on open problems. *arXiv preprint arXiv:2005.01643* .
- Liu, Y., Logan, B., Liu, N., Xu, Z., Tang, J., and Wang, Y. (2017). Deep reinforcement learning for dynamic treatment regimes on medical registry data. In *2017 IEEE International Conference on Healthcare Informatics (ICHI)*, pages 380–385. IEEE.
- Mnih, V., Kavukcuoglu, K., Silver, D., Rusu, A. A., Veness, J., Bellemare, M. G., Graves, A., Riedmiller, M., Fidjeland, A. K., Ostrovski, G., et al. (2015). Human-level control through deep reinforcement learning. *Nature* **518**, 529–533.
- Monrad, J. T. (2020). Ethical considerations for epidemic vaccine trials. *Journal of Medical Ethics* **46**, 465–469.
- Polack, F. P., Thomas, S. J., Kitchin, N., Absalon, J., Gurtman, A., Lockhart, S., Perez, J. L., Pérez Marc, G., Moreira, E. D., Zerbini, C., et al. (2020). Safety and efficacy of the bnt162b2 mrna covid-19 vaccine. *New England Journal of Medicine* **383**, 2603–2615.

- Raghu, A., Komorowski, M., Ahmed, I., Celi, L., Szolovits, P., and Ghassemi, M. (2017). Deep reinforcement learning for sepsis treatment. *arXiv preprint arXiv:1711.09602* .
- Risk, M., Hayek, S. S., Schiopu, E., Yuan, L., Shen, C., Shi, X., Freed, G., and Zhao, L. (2022). Covid-19 vaccine effectiveness against omicron (b. 1.1. 529) variant infection and hospitalisation in patients taking immunosuppressive medications: a retrospective cohort study. *The Lancet Rheumatology* **4**, e775–e784.
- Rutter, C. M., Zaslavsky, A. M., and Feuer, E. J. (2011). Dynamic microsimulation models for health outcomes: a review. *Medical Decision Making* **31**, 10–18.
- Shen, C., Lin, M., Lee, Y., Dong, M., and Zhao, L. (2024). State-of-the-art learning covid-19 vaccine effectiveness using lstm. *Informatics in Medicine Unlocked* page 101561.
- Sherstinsky, A. (2020). Fundamentals of recurrent neural network (rnn) and long short-term memory (lstm) network. *Physica D: Nonlinear Phenomena* **404**, 132306.
- Srivastava, N., Hinton, G., Krizhevsky, A., Sutskever, I., and Salakhutdinov, R. (2014). Dropout: a simple way to prevent neural networks from overfitting. *The journal of Machine Learning Research* **15**, 1929–1958.
- Sun, Q., Jankovic, M. V., Budzinski, J., Moore, B., Diem, P., Stettler, C., and Mougiakakou, S. G. (2018). A dual mode adaptive basal-bolus advisor based on reinforcement learning. *IEEE Journal of Biomedical and Health Informatics* **23**, 2633–2641.
- Sutton, R. S. (1997). On the significance of markov decision processes. In *Artificial Neural Networks—ICANN’97: 7th International Conference Lausanne, Switzerland, October 8–10, 1997 Proceedings 7*, pages 273–282. Springer.
- Sutton, R. S. and Barto, A. G. (2018). *Reinforcement learning: An introduction*. MIT press.

- Tseng, H.-H., Luo, Y., Cui, S., Chien, J.-T., Ten Haken, R. K., and Naqa, I. E. (2017). Deep reinforcement learning for automated radiation adaptation in lung cancer. *Medical Physics* **44**, 6690–6705.
- Van Hasselt, H., Guez, A., and Silver, D. (2016). Deep reinforcement learning with double q-learning. In *Proceedings of the AAAI conference on artificial intelligence*, volume 30.
- Watkins, C. J. and Dayan, P. (1992). Q-learning. *Machine Learning* **8**, 279–292.
- Weltz, J., Volfovsky, A., and Laber, E. B. (2022). Reinforcement learning methods in public health. *Clinical Therapeutics* **44**, 139–154.
- Wu, X., Li, R., He, Z., Yu, T., and Cheng, C. (2023). A value-based deep reinforcement learning model with human expertise in optimal treatment of sepsis. *NPJ Digital Medicine* **6**, 15.
- Yasini, S., Naghibi-Sistani, M., and Karimpour, A. (2009). Agent-based simulation for blood glucose control in diabetic patients. *International Journal of Applied Science, Engineering and Technology* **5**, 40–49.
- Yu, C., Dong, Y., Liu, J., and Ren, G. (2019). Incorporating causal factors into reinforcement learning for dynamic treatment regimes in HIV. *BMC medical informatics and decision making* **19**, 19–29.
- Yu, C., Liu, J., Nemati, S., and Yin, G. (2021). Reinforcement learning in healthcare: A survey. *ACM Computing Surveys (CSUR)* **55**, 1–36.
- Zhang, J. (2020). Designing optimal dynamic treatment regimes: A causal reinforcement learning approach. In *International Conference on Machine Learning*, pages 11012–11022. PMLR.

Supplementary Materials for “Development of COVID-19 booster vaccine policy by micro-simulation and Q-learning”

Guoxuan Ma, Lili Zhao & Jian Kang

S1. Rewards of tabular Q-learning over epochs

We provide the plot of mean running reward over 30 epochs of different vaccine costs for tabular Q-learning in Figure S1. The reward is averaged over all individuals and all time points. The initial policy is never receiving at any time point for all vaccine costs. For all vaccine costs, the mean reward converges before 30 epochs, showing that training the Q-learning algorithm for 30 epochs is sufficient.

S2. Convergence and stability issues of deep Q-learning

In Figure S2, we present the average reward over individuals along 30 epochs for deep Q-learning, considering various neural network architectures and learning rates, as well as the average reward for tabular Q-learning. The deep Q-learning models utilize networks with two hidden layers, each containing either 64 or 256 nodes. For each architecture, we consider two learning rates, 10^{-3} and 10^{-4} , with the Adam optimizer (?). For instance, in Figure ??, the line with label “deep Q 64-4” corresponds to a Q-network of two hidden layers with 64 nodes each, trained by the Adam optimizer with learning rates 10^{-4} .

Figure S2 shows that deep Q-learning suffers from convergence difficulties and stability issues for all combinations of architectures and learning rates. The Q-network with two layers of 256 nodes and trained with learning rate 10^{-3} (deep Q 256-3) converges when vaccine cost is 0.001, but does not converge for other vaccine costs. Similarly, the Q-network with two layers of 64 nodes, trained with learning rate 10^{-3} (deep Q 64-3), converges only when vaccine cost is 0.01. The Q-network with two layers of 64 nodes and trained with learning rate 10^{-4} (deep Q 64-4) converges only when vaccine cost is 0.04. The same Q-network architecture trained

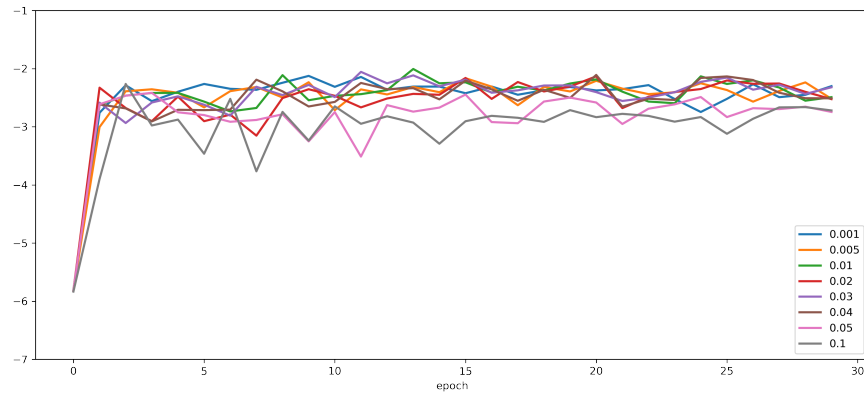


Figure S1. The mean running reward ($\times 10^{-4}$) over 30 epochs of different vaccine costs for tabular Q-learning.

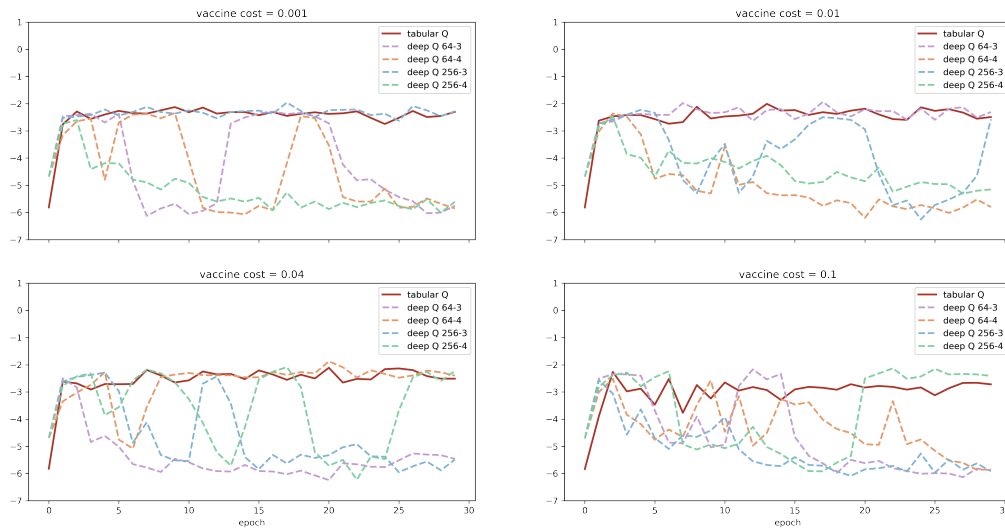


Figure S2. The mean running reward ($\times 10^{-4}$) over 30 epochs of different vaccine costs for tabular Q-learning and deep Q-learning with different architectures and learning rates.

with the same learning rate exhibits highly variable performance depending on the vaccine cost. Even when deep Q-learning converges, its has similar reward compared to that of tabular Q-learning. In contrast, tabular Q-learning consistently converges and demonstrates robust performance. This shows the practical advantage of tabular Q-learning over deep Q-learning in this application.